JOURNAL OF MORPHOLOGY 267:555–568 (2006)

Confocal Microscopy of the Light Organ Crypts in Juvenile *Euprymna scolopes* Reveals Their Morphological Complexity and Dynamic Function in Symbiosis

Laura K. Sycuro, Edward G. Ruby, and Margaret McFall-Ngai*

Department of Medical Microbiology and Immunology, University of Wisconsin, Madison, Wisconsin 53706

ABSTRACT In the hours to days following hatching, the Hawaiian bobtail squid, *Euprymna scolopes,* obtains its light-emitting symbiont, *Vibrio fischeri*, from the surrounding environment and propagates the bacteria in the epithelial crypts of a specialized light organ. Three-dimensional analyses using confocal microscopy revealed that each of the three crypts on either side of the juvenile light organ is composed of four morphological regions. Progressing from the lateral pore to the medial blind end of each crypt, the regions consist of 1) a duct, 2) an antechamber, 3) a bottleneck, and 4) a deep region. Only the deep region houses a persistent bacterial population, whereas the duct, antechamber, and bottleneck serve as conduits through which the bacteria enter during initial colonization and exit during diel venting, a behavior in which ~90% of the symbionts are expelled each dawn. Our data suggest that, like the duct, the antechamber and bottleneck may function to promote and maintain the specificity of the symbiosis. Pronounced structural and functional differences among the deep regions of the three crypts, along with previously reported characterizations of embryogenesis, suggest a continued developmental progression in the first few days after hatching. Taken together, the results of this study reveal a high degree of complexity in the morphology of the crypts, as well as in the extent to which the three crypts and their constituent regions differ in function during the early stages of the symbiosis. J. Morphol. 267:555–568, 2006.

KEY WORDS: *Euprymna scolopes*; *Vibrio fischeri*; symbiosis; light organ,; confocal microscopy

A juvenile *Euprymna scolopes* squid (Cephalopoda:Sepiolidae) emerges from its egg poised to recruit cells of its luminous bacterial symbiont, *Vibrio fischeri*, from the surrounding seawater into nascent light organ tissues (for review, see Nyholm and McFall-Ngai, 2004). Although *V. fischeri* constitutes less than 0.1% of the microbial population in ambient seawater, the hatchling squid acquire a monospecific culture of this species of luminous bacteria in as little as 12 h (McFall-Ngai and Ruby, 1991; Ruby and Lee, 1998). Even in the absence of the symbiont, other environmental bacteria do not colonize the light organ (McFall-Ngai and Ruby, 1991). Once initiated, the squid will maintain the symbiosis with a high degree of specificity throughout its life, apparently using the bacterial luminescence for counterillumination defense against predation (Moynihan, 1983). Each morning at dawn the squid vents ~90% of its symbionts, allowing the remaining cells to grow up into a healthy, luminescent culture by evening (Boettcher et al., 1996).

The biological mechanisms by which the squid establishes and sustains symbiosis are remarkably complex and highly localized (Nyholm and McFall-Ngai, 2004). The single light organ in the center of the hatchling squid's body cavity (Fig. 1A) provides the stage for the diverse and highly specialized functions of symbiont collection, colonization, and propagation, as well as the determination of specificity and the control of bacterial luminescence. The tissues that mediate these complex processes develop both embryonically and postembryonically (Montgomery and McFall-Ngai, 1998).

Embryogenesis creates a nascent light organ in the hatchling that functions to ensure colonization by the proper symbiont species (Montgomery and McFall-Ngai, 1993; Nyholm et al., 2000; Nyholm et al., 2002; Nyholm and McFall-Ngai, 2003). The bilateral organ is roughly heart-shaped (Fig. 1B) and its dimensions average 500–600 μm laterally and 400–500 μm along the anterior–posterior axis

Contract grant sponsor: National Science Foundation (NSF); Contract grant number: IOB-0517007; Contract grant sponsor: National Institutes of Health (NIH); Contract grant numbers: RR-12292, AI-50661; Contract grant sponsor: WM Keck Foundation.

Present address for L.K. Sycuro: Department of Microbiology, University of Washington, and Department of Human Biology, Fred Hutchinson Cancer Research Center, Seattle, WA 98109.

*Correspondence to: Margaret McFall-Ngai, Department of Medical Microbiology and Immunology, University of Wisconsin, 1300 University Ave., Madison, WI 53706. E-mail: mjmcfallngai@wisc.edu

Published online 20 January 2006 in
Wiley InterScience (www.interscience.wiley.com)
DOI: 10.1002/jmor.10422

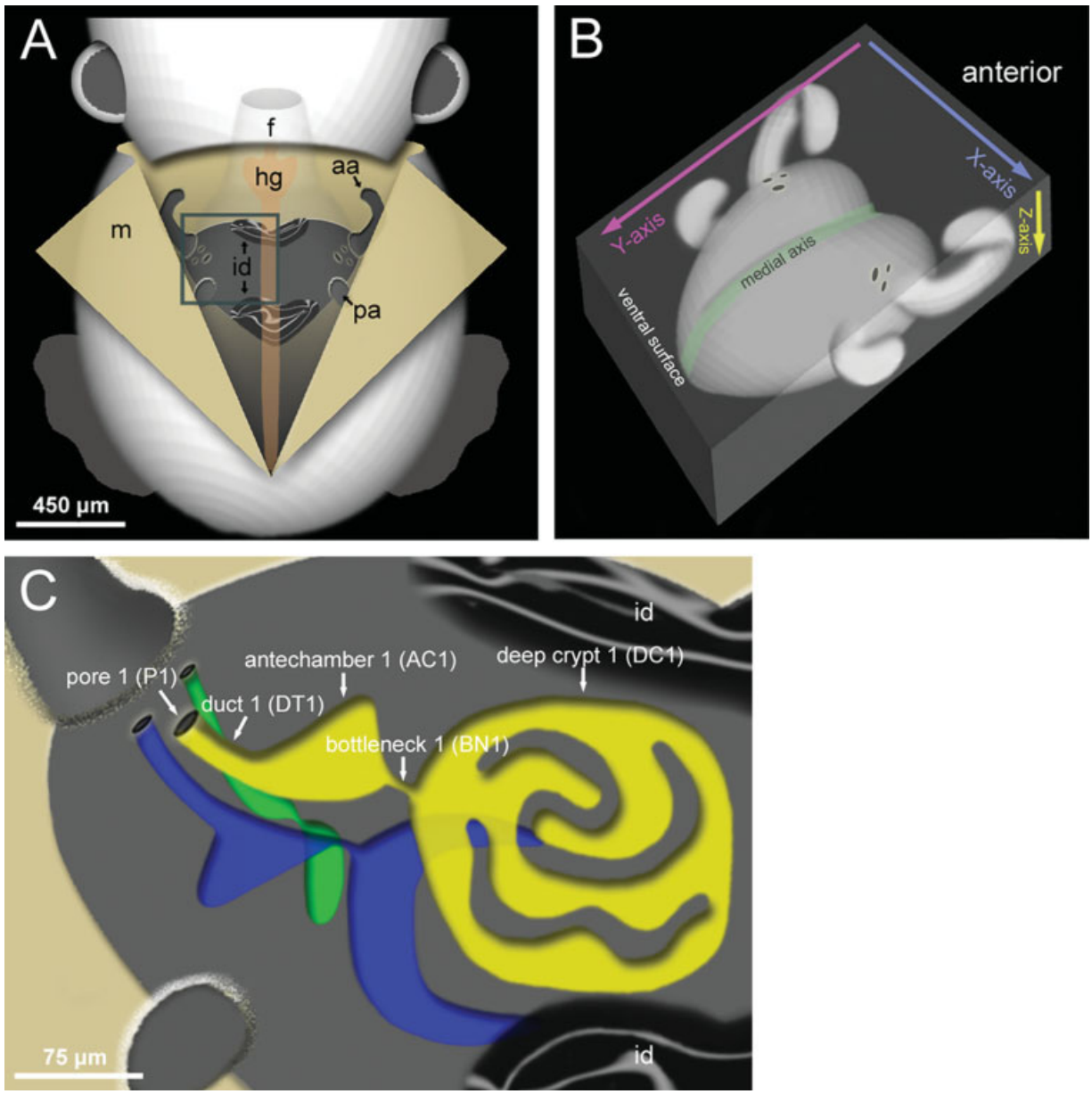

Fig. 1. Diagrammatic representations of the juvenile *Euprymna scolopes* light organ and its internal crypts to provide an orientation for subsequent confocal images. **A:** Ventral dissection of a juvenile squid's mantle (m) revealing the light organ in the central body cavity, invested in the posterior opening of the funnel (f) and dorsal to the hindgut (hg, orange). The anterior appendage (aa) and posterior appendage (pa) are laterally located projections of ciliated epithelium that arch over the three pores and assist in the initial collection of symbiotic bacteria. The ink sac covers the dorsal surface of the light organ and the diverticula of the ink sac (id) extend across the ventral surface of the organ at the anterior and posterior edges. The precise arrangement of these diverticula varies from that shown to an extended position covering much of the ventral surface of the organ. The orientation in this panel and all subsequent figures is anterior to the top, unless otherwise noted. **B:** A 3D rendering of the light organ after being dissected and removed from the mantle cavity. The image illustrates the overall shape and relationship of external features, as well as the progression of confocal serial sections through the organ, all of which were taken ventral to dorsal along the Z axis. **C:** A detailed view of the internal components of one half of a representative juvenile light organ, illustrating the position and general morphology of the internal crypts (area shown is that circumscribed by the box in **A**). The oldest to the most recently developed crypts, respectively, are designated crypt 1 (yellow), crypt 2 (blue), and crypt 3 (green). The four morphological regions (duct, DT; antechamber, AT; bottleneck, BN; and deep crypt, DC) shared by all three crypts are labeled only on crypt 1 for clarity.

(Montgomery and McFall-Ngai, 1993). Superficially, the most striking morphological features of the hatchling light organ are lateral ridges of ciliated epithelia and two ciliated epithelial appendages that extend from each ridge (McFall-Ngai and Ruby, 1991; Montgomery and McFall-Ngai, 1993). The ring-like shape created by each pair of appendages, in conjunction with the ciliary currents they pro-

duce, promote the gathering of *Vibrio fischeri* from the ambient seawater (Nyholm et al., 2000). Inside the nascent light organ are six epithelial crypts that are arranged in two groups of three (Fig. 1C), with symmetry about the sagittal plane. On each side of the light organ the three crypt spaces are designated crypts 1, 2, and 3 to indicate the order in which they develop during embryogenesis (Montgomery and McFall-Ngai, 1993). Each crypt has a ciliated duct leading to a pore at the surface of the light organ. The outward beating of the duct cilia, along with the presence of an oxidatively stressful environment in the duct, suggest that this region plays a role in controlling bacterial specificity (McFall-Ngai and Ruby, 1998; Davidson et al., 2004).

Almost immediately after successful colonization by the proper symbiont, the early postembryonic light organ develops anatomically and morphologically into the mature light organ that will support a persistent *Vibrio fischeri* infection throughout the life of the squid. Within 12 h of entering the crypts the bacterial symbionts deliver a signal that induces the loss over the subsequent 5 days of both the superficial ciliated field and the appendages (Montgomery and McFall-Ngai, 1994; Doino and McFall-Ngai, 1995). Other aspects of superficial light-organ morphology that change dramatically in the first several days to weeks following hatching are symbiosis-independent, or "preprogrammed," and occur even in aposymbiotic (uncolonized) animals. Notably, the ink sac, which is located immediately dorsal to the light organ, extends diverticula around the light organ (first anteriorly and posteriorly, and then laterally) to form retractable iris-like structures over the ventral surface that control the amount of light emitted (Montgomery and McFall-Ngai, 1998). Further, the tissues comprising the reflectors, lenses, and yellow filters mature and begin to function in modulating light emission, and the morphology of the light organ itself changes into the bilobed structure characteristic of the adult squid (Montgomery and McFall-Ngai, 1998).

Examples of both symbiosis-specific and preprogrammed morphological development also take place in the crypts. Two changes occurring within the first 24 h of colonization are symbiosis-dependent, and can be reversed by antibiotic treatment that eliminates the bacteria: 1) a change in crypt epithelial cell morphology from columnar to cuboidal (Montgomery and McFall-Ngai, 1994; Visick et al., 2000); and 2) the induction of an increase in the abundance of microvilli along the apical surface of the crypt epithelia (Montgomery and McFall-Ngai, 1994; Lamarcq and McFall-Ngai, 1998). In combination, these alterations result in a greater degree of physical contact between host epithelial cells and the bacterial symbionts that fill the crypt spaces. The subsequent development of the crypts is preprogrammed and consists of an increase in both the volume of the crypts and the extent of crypt branching (Montgomery and McFall-Ngai, 1998; Claes and Dunlap, 2000). Additionally, the three pores and three ducts on each lateral side of the organ coalesce into a single pore and single duct, irrespective of whether colonization has occurred (Montgomery and McFall-Ngai, 1998).

In this study we used confocal microscopy to derive an in-depth characterization of the morphology and anatomy of the three-dimensionally complex postembryonic light organ. Our analyses reveal new internal features of the organ that appear to serve critical functions in the symbiosis. In addition, we provide new information about the role of symbiosis in the developmental events that transform the organ from a structure that promotes colonization to one that fosters persistence of the beneficial association.

MATERIALS AND METHODS

General Procedures

Adult *Euprymna scolopes* (Cephalopoda:Sepiolidae) were collected from shallow sand flats on the south shore of Oahu, HI. The animals were housed in running seawater aquaria and females were mated once a week. The resulting egg clutches were transferred to a 23°C recirculating aquarium with a 12h:12h light/dark cycle in which they were maintained until hatching.

Newly hatched juveniles were immediately removed from the egg tanks and placed in *Vibrio fischeri*-free seawater (WSW; i.e., seawater that contains a variety of bacteria at a concentration of $\sim 10^5$–10^6 cells/ml, but does not contain detectable levels of *V. fischeri*). Unless otherwise noted, only squid on or after developmental Stage A30 (Arnold et al., 1972), i.e., when all three crypts are present, were used in these experiments. To produce symbiotic juveniles, a subset of hatchlings were inoculated with cultures of the wildtype *V. fischeri* strain ES114 that had been grown at 28°C to mid-logarithmic phase in a seawater-based tryptone medium (SWT) (Boettcher and Ruby, 1990). For experiments in which the bacterial symbionts were to be observed with confocal microscopy, the *V. fischeri* cells carried the multicopy plasmid pKV111, which encodes both the gene for a red-shifted GFP derivative and a chloramphenicol (CM) antibiotic-resistance marker (Nyholm et al., 2000). The plasmid was maintained by adding CM (5 μg/ml) to the SWT culture medium and to the WSW containing the symbiotic squid (1 μg/ml); previous studies have shown that CM at these levels does not markedly alter the colonization process (unpubl. data). A fresh culture of *V. fischeri* was diluted in WSW to a final concentration of 10^3–10^4 colony-forming units (CFU) per ml and newly hatched squids were placed in individual scintillation vials containing 4 ml of this inoculum for a period of 3 or 12 h. The animals were then transferred into fresh *V. fischeri*-free WSW and

each day thereafter for the duration of the experiment. After 24 h the luminescence output of each squid was measured with a Turner 20/20 luminometer (Turner Designs, Sunnyvale, CA) to confirm that it was either symbiotic or aposymbiotic.

Confocal Microscopy

When possible, the light organ was fixed and permeabilized prior to fluorochome staining because this pretreatment promoted a relatively uniform stain penetration, even in the deeper portions of the crypts. At appropriate timepoints, squid were anesthetized in a solution of 2% ethanol in seawater that had been passed through a 0.2-μm pore-sized filter (FSW). The mantle and funnel tissues were dissected away and the animal was placed for 1 h at room temperature in marine phosphate-buffered saline (mPBS; 0.45 M NaCl in a 50 mM sodium phosphate buffer, pH 7.4) containing 4% formaldehyde. The squid were washed in mPBS before the light organs were isolated by dissection and the ink sac was pierced on the dorsal side to facilitate the draining of ink. The dissected light organs were then rinsed in mPBS again and permeabilized in a solution of 1% Triton X-100 for 20 min. Light organs were then stained with BODIPY-FL paclitaxel and/or rhodamine phalloidin. Paclitaxel, which stains tubulin, was used at a concentration of 20 μg/ml in mPBS to which 0.5% Triton X-100 had been added. Phalloidin, which stains F-actin, was used at ~165 nM, also in mPBS containing 0.5% Triton X-100. For each stain the light organs were incubated in the dark for 20 min, followed by two washes in mPBS. The light organs were mounted individually on flat slides in a medium consisting of 95% glycerol, 5% mPBS, and 5 mg/ml paraphenylenediamine, a reagent that slows the fading of fluorochromes. All fluorochromes were purchased from Invitrogen (Carlsbad, CA) unless otherwise noted.

Some confocal analyses of crypt morphology and bacterial localization were conducted using live animals. For studies of early stages of colonization, juvenile squid were incubated in WSW containing 0.001% CellTracker Orange for 15–30 min. For later timepoints, the incubation time in 0.001% CellTracker Orange was 12–24 h, beginning 12 h after colonization. After staining, the squid were rinsed in WSW and anesthetized in FSW containing 2% ethanol. The mantle and funnel were dissected away to expose the underlying light organ (Fig. 1A) and the animal was mounted on a depression slide.

The squid, or their dissected light organs, were mounted ventral side up and oriented anterior to the top. All confocal Z-series images were taken in a ventral-to-dorsal sequence (Fig. 1B). A Zeiss (Thornwood, NY) LSM510 laser-scanning confocal microscope was used to collect digital images, which were processed using Zeiss software and Adobe Photoshop (San Jose, CA) Elements.

Measurements

All quantitative measurements were taken using the Zeiss LSM510 software. Measurements of the light organ or crypt regions taken along the X, Y, and Z axes were designated length, width, and depth, respectively (Fig. 1B). The cross-sectional area of each crypt region was approximated by determining the maximal length (x) and width (y) measurements, and using these values to calculate the area of an ellipse: $\text{area}_{\text{ellipse}} = (0.5x)(0.5y)(\pi)$.

All quantitative studies of individual epithelial cells were conducted using both fluorescein-conjugated paclitaxel for cytoplasmic staining and rhodamine phalloidin to stain the actin cytoskeleton; the cell nuclei were unstained. The precise location of the cell membrane could not be resolved, so cell width measurements were made along the apical surface (brush border), which stained vividly with rhodamine phalloidin, applying the assumption that the membrane border between two cells was situated halfway between their nuclei. Cell height measurements were taken from the tip of the red-staining apical brush border to the basal edge of the bright-green-staining cytoplasm.

RESULTS

Crypt Morphology

While the three epithelial crypts on either side of the juvenile *Euprymna scolopes* light organ do not appear identical, they each have the same four morphological regions: 1) duct (DT), 2) antechamber (AC), 3) bottleneck (BN), and 4) deep crypt (DC) (Figs. 1C, 2, 3). These four crypt regions were apparent in all ($n > 100$) juvenile squid observed in this study, regardless of whether they were colonized with symbionts. The following is a brief description of the morphology of each region in newly hatched animals. We provide detailed descriptions of crypt 1, the largest and most structurally complex, and crypt 3, the smallest and most rudimentary; both the size and the morphology of crypt 2 are intermediate to the other two crypts. The reported measurements were purposely combined from squid that had hatched from several different clutches, but in all cases the animals were less than 3 h posthatch (for each measurement, $n = 10$). Live and fixed animals showed similar crypt dimensions and morphologies.

Duct. As described in a previous publication (Montgomery and McFall-Ngai, 1993), the most lateral segment of each crypt is a tube-like, ciliated duct that extends medially from the superficial pore (Figs. 1C, 2). The duct of crypt 1 (DT1) has the largest cross-sectional area (average = 163 ± 21 μm^2 standard error of the mean, SEM), and is the shortest in length (average = 27 ± 3.3 μm SEM). It connects to the most ventral antechamber. Conversely, DT3 has the smallest cross-sectional area

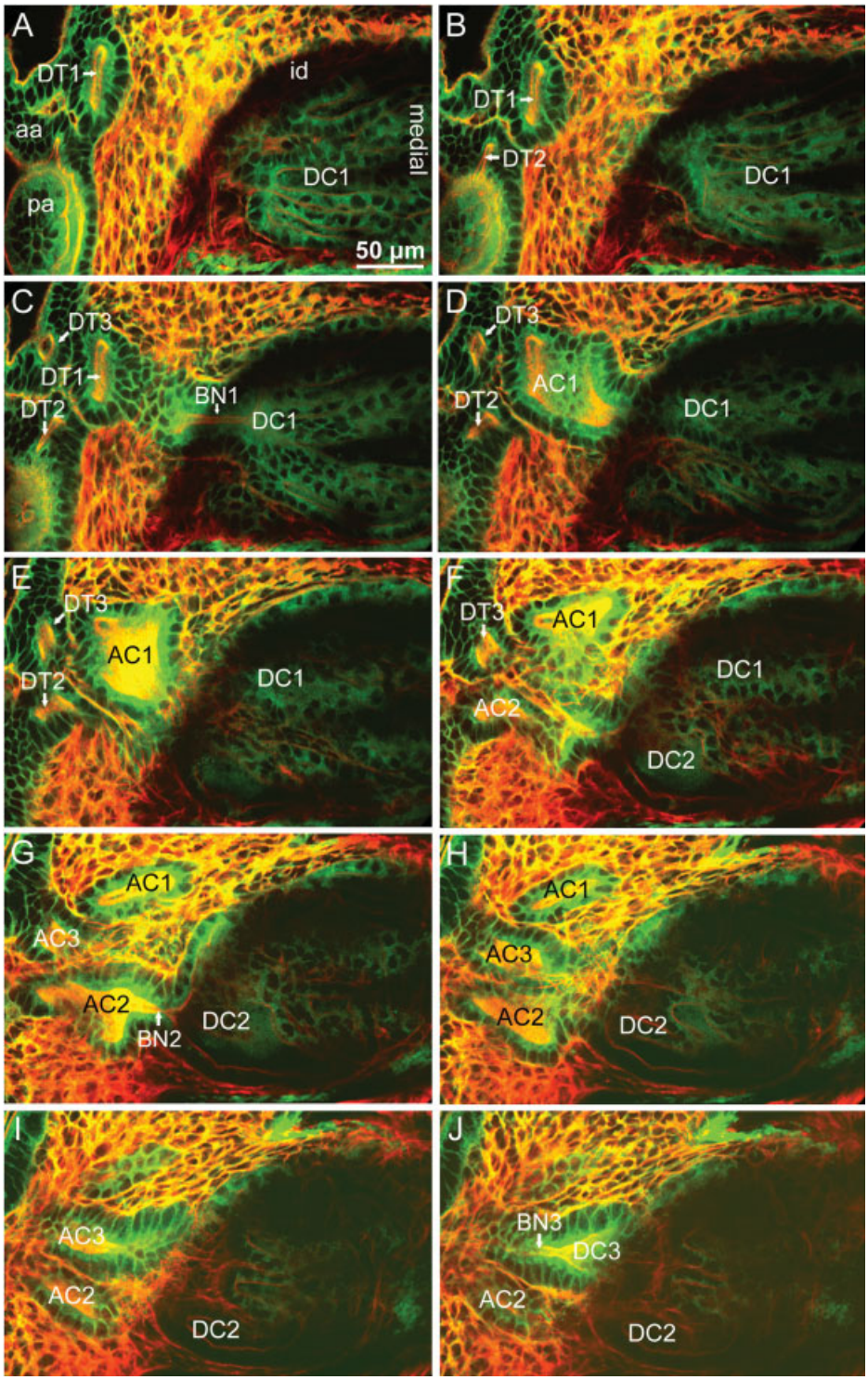

Fig. 2. Three-dimensional relationships of the regions of the crypts. A confocal series through the Z axis of the light organ of a typical juvenile *Euprymna scolopes*, showing the relationship of the four crypt regions for each of the three crypts. To illustrate these features and provide details of cell size and shape, the organ of a 48-h aposymbiotic (i.e., uncolonized) animal was stained with rhodamine phalloidin, which labels filamentous actin (red), and BODIPY-FL paclitaxel, which labels tubulin in the cytoskeleton (green). Digital images of sections at 3.9-µm intervals, beginning at the ventral surface (see Fig. 1B), are arrayed in sequence in **A–J**. aa, anterior appendage of superficial ciliated field; AC1, AC2, AC3, antechamber of crypt 1, 2, 3; BN1, BN2, BN3, bottleneck of crypt 1, 2, 3; DC1, DC2, DC3, deep crypt 1, 2, 3; DT1, DT2, DT3, duct of crypt 1, 2, 3; id, ink sac diverticulum; pa, posterior appendage of superficial ciliated field.

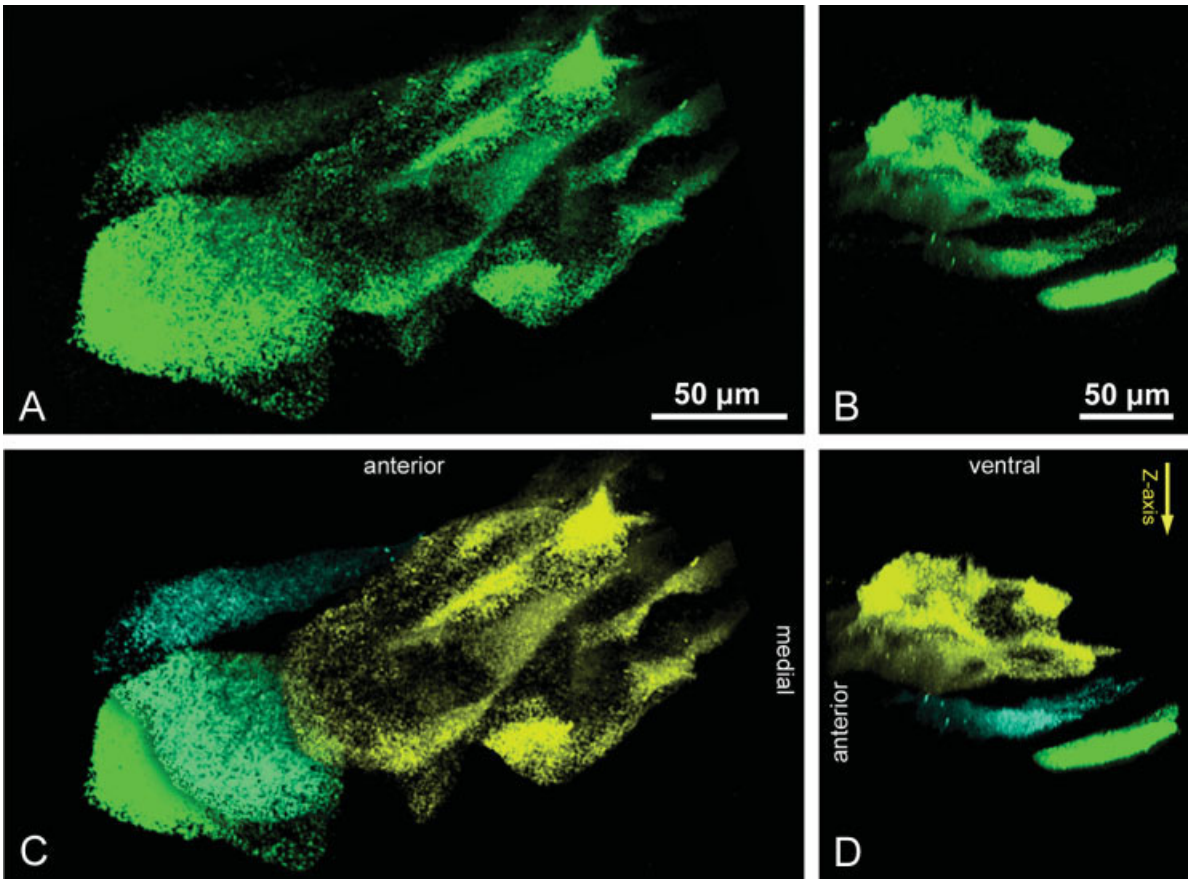

Fig. 3. The deep crypt regions, where the symbionts persistently reside. Three-dimensional projections of a confocal series taken at 1.4-μm intervals through the Z axis of the deep crypts of a 48-h symbiotic juvenile *Euprymna scolopes* colonized by GFP-labeled *Vibrio fischeri*, revealing the sizes, shapes, and relative positions of the deep crypt lumina. **A,B:** Images of the GFP-labeled *V. fischeri* filling the deep crypt lumina. **A:** Projection looking through the Z axis, ventral to dorsal. **B:** Image of **A** rotated around the Y-axis ~90° and reoriented so ventral is to the top. Perspective is looking through the X axis, lateral to medial. **C,D:** The projections in **A** and **B** viewed in stereo, and false-colored to differentiate the three crypt spaces; crypt 1, yellow; crypt 2, blue; crypt 3, green.

(average = 64 ± 6.9 μm^2 SEM), and longest length (average = 36 ± 5.0 μm SEM), connecting to the most dorsal antechamber.

Antechamber. Medial to the duct is a large compartment that we have named the antechamber. The antechamber of crypt 1 (AC1) begins as a gradual widening of the duct and eventually opens into a stomach-shaped cavity that is often ciliated. This main compartment of AC1 has a large cross-sectional area averaging 1,380 ± 150 μm^2 SEM (Figs. 1C, 2), but is very shallow, with a narrow dorsal out-pocketing that extends several micrometers. In contrast to AC1, AC3 is little more than a widening of the duct, with the largest portion measuring, on average, only 510 ± 64 μm^2 SEM in cross-sectional area.

Bottleneck. The bottleneck is a short and narrow connector between the antechamber and the deep crypt region (Figs. 1C, 4B,C). The bottleneck of crypt 1 (BN1) in a hatchling squid is 8.9 ± 0.6 μm SEM in width and 32 ± 1.6 μm SEM in length. BN3 is smaller, measuring only 5.4 ± 0.3 μm SEM in width and 16 ± 1.4 μm SEM in length. Cilia were never observed on the cells of this region.

Deep crypt. Farthest from the pore, the blind-ended deep-crypt region is the most voluminous portion of the crypt (Fig. 1C). Among the three deep crypts, deep crypt 1 (DC1) is the largest and has the most structural complexity. DC1 is also the most medial of the deep crypts and the only one that extends ventrally from the bottleneck, almost reaching the ventral surface of the light organ (Figs. 2, 3D). DC1 first opens up into one large compartment, which usually splits into three primary diverticula (Fig. 1C). These diverticula have irregular morphologies with many branches and out-pocketings, but at the medial axis they reconnect into a single space. Due to the convoluted structure of DC1, it was not possible to estimate its volume, but we determined that its length, from the bottleneck to the medial axis, averages 175 ± 8.5 μm SEM. By comparison, DC3 is less complex in the hatchling, usually occurring as a single round or ellipsoidal compartment

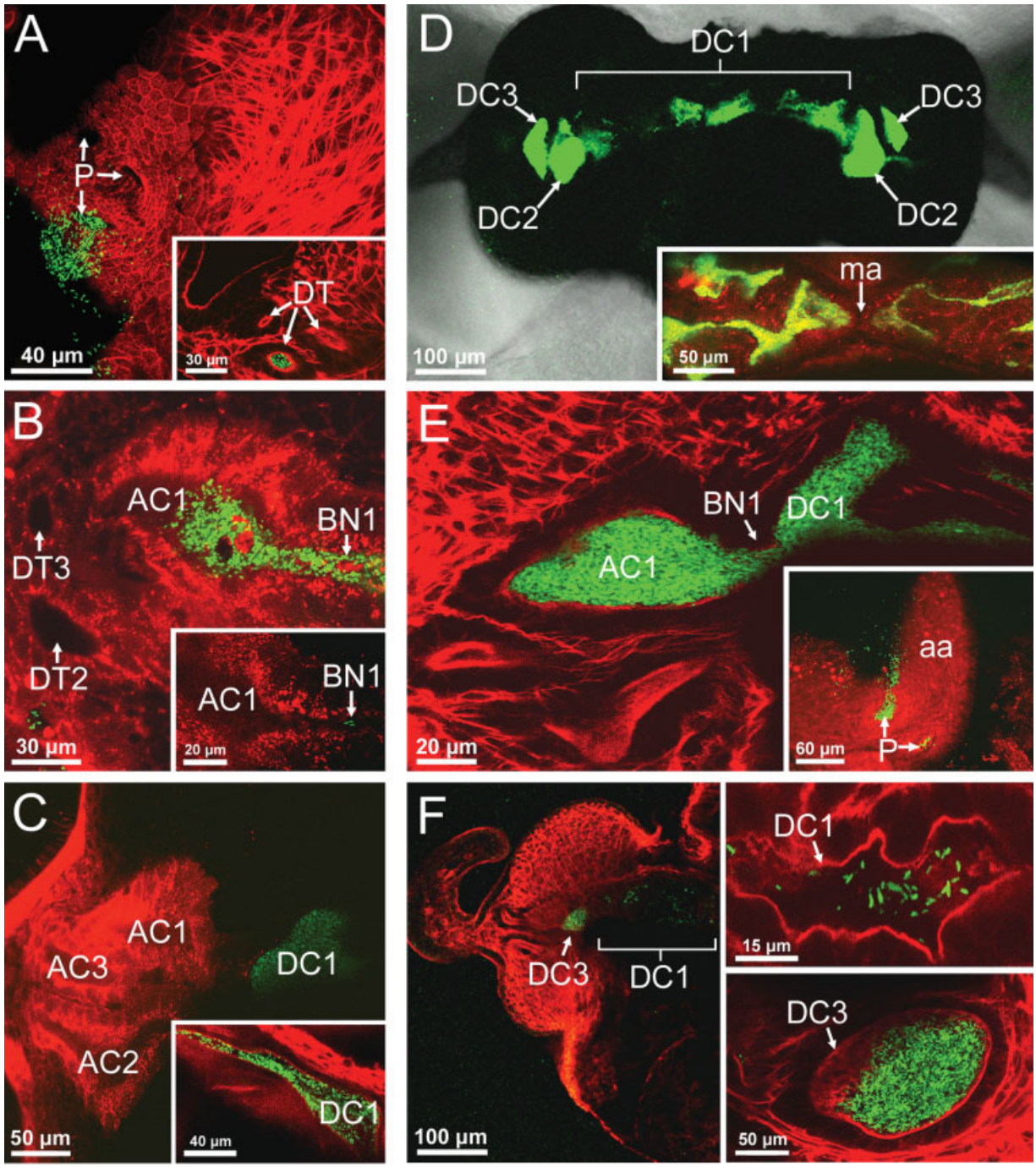

Fig. 4. The location of *Vibrio fischeri* cells over the first 72 h following inoculation of the juvenile host. Light organs of juvenile *Euprymna scolopes* were counterstained with either rhodamine phalloidin or CellTracker Orange to visualize the relationship of host tissues (red) to GFP-labeled *V. fischeri* cells (green). **A:** As previously described (Nyholm et al., 2000), between 0–4 h bacteria were observed in large aggregates above the light organ pores, as well as in the ducts (inset). **B:** Between 4–8 h symbiont populations were often observed in crypt antechambers and bottlenecks, sometimes passing through these structures in large numbers, while at other times numbering only a few bacterial cells at a time (inset). **C:** By 17 h, populations of symbiont cells had migrated to the deep crypts and grown to fill the deep crypt lumina, with large populations of bacteria extending laterally to the bottleneck and medially through the deep crypt diverticula to the medial axis (inset). **D:** The light organ locations of symbiotic bacteria in the evening, at which time they were confined to the deep crypts. Higher magnification of the blind ends of the opposing DC1 regions that meet, but do not join, at the medial plane (inset). **E:** During diel venting at dawn, the bacteria could be seen reentering the antechambers through the bottlenecks. Bacterial populations were subsequently observed exiting the pores into the mantle cavity (inset). **F:** Immediately following venting, small populations of *V. fischeri* cells remained in the most mature crypt (DC1; inset, upper right), but often large populations remained in the least mature of the crypts (DC3; inset, lower right). aa, anterior appendage of superficial ciliated field; AC1, AC2, AC3, antechamber of crypt 1, 2, 3; BN1, BN2, BN3, bottleneck of crypt 1, 2, 3; DC1, DC2, DC3, deep crypt 1, 2, 3; DT, ducts; DT2, DT3, duct of crypt 2, 3; ma, medial plane of the light organ; P, pores.

that averages only 16 ± 3.6 μm SEM in length (Fig. 3D).

Localization of *Vibrio fischeri* Within the Crypts During Primary Colonization and Early Persistence

While primary colonization of the juvenile light organ crypts has a very high success rate, many aspects of the process are variable. In a typical newly hatched animal there is no particular order in which the six crypts become colonized, nor does the sequence of events over the first hours to days follow a rigid timeline. As previously reported (Nyholm et al., 2000), during the first 4 h of exposure to *Vibrio fischeri* the bacteria are predominately outside the light organ, aggregating in groupings of various cell numbers in the mucus shed by the cells of the superficial ciliated field (Fig. 4A). Using GFP-labeled *V. fischeri* we could observe the bacteria entering the ducts as early as 2 h after inoculation (Fig. 4A, inset), and first entering the antechamber, bottleneck, and deep-crypt regions between 4 and 8 h after inoculation. In some instances, large populations of bacteria migrate en masse through the antechamber and bottleneck (Fig. 4B), but at other times the bacteria appear to colonize in smaller groups of 2–20 cells (Fig. 4B, inset). In either case, the bacteria negotiate the duct, antechamber, and bottleneck, apparently without any detectable delay or accumulation in the antechamber. On occasion, we observed bacteria streaming straight through the antechamber to the bottleneck. By 17 h postinoculation many light organs are fully colonized, i.e., all six deep crypts contain large numbers of bacteria, while others are still undergoing colonization in one or several crypts. The deep crypts that do contain bacteria at 17 h are usually full, while their corresponding antechambers and bottlenecks have become devoid of bacteria (Fig. 4C).

Under our experimental conditions, essentially 100% of inoculated squid were colonized by 24 h. After this time the spatial pattern of the symbiont population becomes dominated by the host's diel expulsion behavior. Each evening (i.e., at 24, 48, and 72 h postinoculation), large populations of symbiotic bacteria can be found exclusively in the deep regions (Fig. 4D); when bacteria are observed in the duct, antechamber, or bottleneck, they generally number fewer than 10 cells. Just before dawn (i.e., immediately preceding the environmental light cue that results in the expulsion of most of the symbiont population), the distribution of bacteria within the crypts is identical to that of the preceding evening. However, between 10 and 40 min after light exposure and expulsion, the bacteria are typically seen in large quantities throughout all four crypt regions (Fig. 4E), and are spilling out of the light organ through the pores (Fig. 4E, inset). At least a few bacteria are generally seen in the duct region of each crypt, indicating that all of the deep crypts expel their symbionts. However, the extent to which expulsion clears this region varies; typically, DC1 is nearly emptied, DC2 expels the majority of its bacteria, but not as much as DC1, while DC3 expels very few cells and still appears essentially full (Fig. 4F). Within 4–5 h following expulsion the remaining symbionts have rapidly proliferated in the deep regions and bacterial cells can no longer be detected in the ducts, antechambers, or bottlenecks.

Symbiont-Induced Changes in the Morphology and Anatomy of the Crypt Region

The morphological responses of the ducts to interactions with *Vibrio fischeri*, including a symbiosis-induced constriction, have been previously reported (Kimbell and McFall-Ngai, 2004); thus, an analysis of this region is not covered here. In contrast, our examination of the antechambers revealed no detectable morphological or anatomical differences in response to symbiosis or development during the first 72 h posthatch. The minimum diameter of the bottleneck, however, decreases during the first 72 h after hatching. While some narrowing occurs in bottlenecks 1 and 2 of aposymbiotic animals, the bottlenecks of all three crypts constrict significantly ($P \leq 0.01$) in symbiotic animals, measuring only 2–4 μm in diameter by 48 h (Fig. 5). The length of the bottleneck does not change significantly either with time or with symbiotic state (data not shown).

Our discovery that the deep region is the only part of each crypt in which host epithelial cells continually interact with *Vibrio fischeri* led us to investigate whether the reversible, symbiosis-induced change in epithelial cell morphology (Montgomery and McFall-Ngai, 1994; Visick et al., 2000) is restricted to the deep region and, if it is, whether the change is equally apparent in all crypts. In three replicate experiments we visually and quantitatively observed the typical columnar to cuboidal change in cell morphology in symbiotically colonized DC1 epithelia at 48 h (Fig. 6). In contrast, no detectable change in the dimensions of the epithelial cells lining either the antechamber or the bottleneck was induced by symbiosis (data not shown). In similar experiments with DC2, no alteration in epithelial cell morphology was detected in two out of three experiments. In the third experiment, the height-to-width ratio of the symbiotic DC2 epithelial cells was ~1.5, suggesting that these cells were in the process of changing from columnar to cuboidal. Finally, in fully colonized DC3 the epithelial cells were columnar, i.e., indistinguishable from those of aposymbiotic animals. Thus, we conclude that, in this early stage of the symbiosis, the DC regions respond differently to the presence of bacterial symbionts, depending on their developmental maturity.

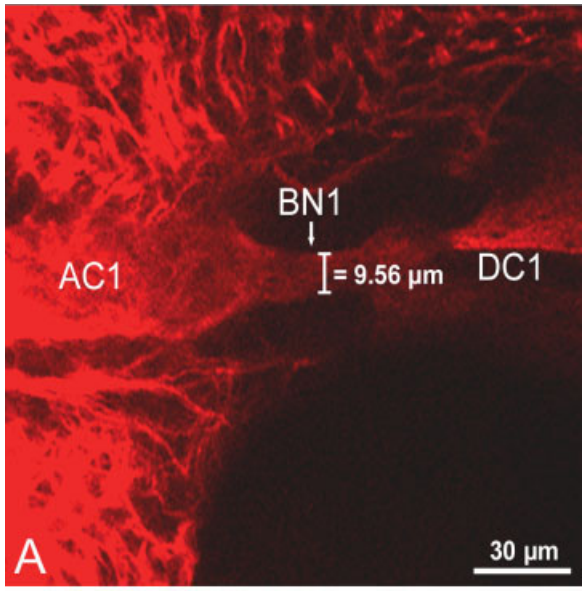

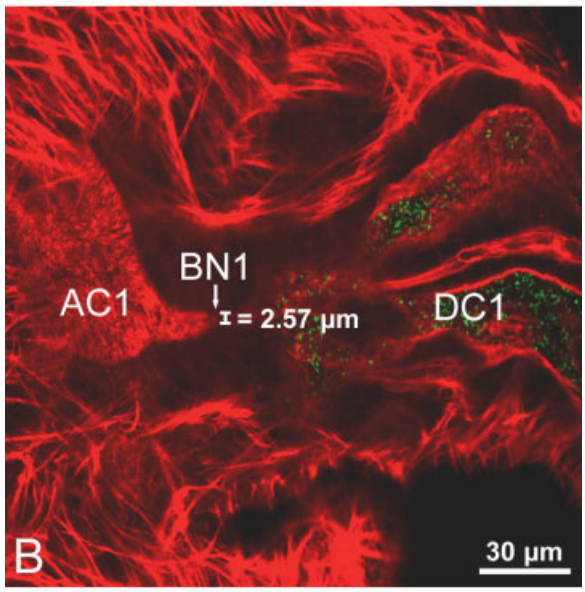

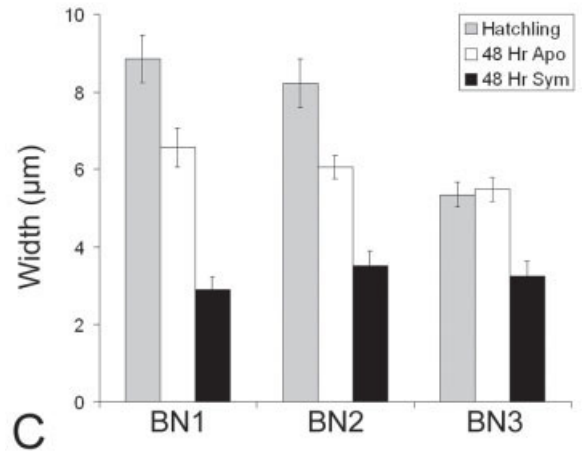

Developmental Morphology of Deep Crypts 2 and 3

Differences in the development of the deep crypts were examined in symbiotic and aposymbiotic animals imaged at 24-h intervals from hatching through 72 h. The shape of the deep-crypt lumen was outlined by counterstaining with either rhodamine phalloidin or CellTracker Orange. To maximize the range of developmental differences possible for posthatch animals during the relatively short 72-h time frame, we collected data from animals hatched from four independent clutches. Of the four clutches analyzed in this experiment, two hatched before Stage A30, i.e., somewhat premature and after crypt 3 had just begun formation, and two were from clutches that were at or beyond A30, i.e., at a developmental stage typical of the normal hatchling (Arnold et al., 1972; Montgomery and McFall-Ngai, 1993). No progressive developmental pattern was observed in the morphology or size (length and width) of DC1 in the first 72 h, nor was there any detectable change induced by symbiosis. However, there was a developmental progression in the observed morphologies of DC2 and DC3 that consisted of four identifiable stages (Fig. 7). Overall, most juvenile squid are in either Stage 2 or Stage 3 during the first 72 h after hatching. Stage 1 is seldom encountered, but when observed, it is nearly always in a newly hatched animal, suggesting that this stage is a morphological characteristic of an earlier period of development. Similarly, when Stage 4 is observed the animal is always 48 h posthatch, suggesting that it represents a more advanced developmental stage. Throughout the progression, DC2 is larger and essentially one stage ahead of DC3. Like DC1, DC2 is also readily colonized by *Vibrio fischeri* regardless of its developmental stage at hatching. DC3, on the other hand, is usually not colonized if it is still at Stage 1, but always becomes colonized if it has progressed to a later developmental stage. In general, symbiosis appears to have little if any impact on the developmental morphology of DC2 and DC3; however, they were significantly larger in cross-sectional area ($P \leq 0.02$) in symbiotic animals than in aposymbiotic animals of the same age (data not shown).

Fig. 5. Developmental and symbiosis-induced changes in the crypt bottleneck. **A:** A representative bottleneck of a newly hatched animal. **B:** Bottleneck of a 48-h symbiotic juvenile *Euprymna scolopes* from the same clutch, colonized with GFP-labeled *Vibrio fischeri*. In both images the actin-rich epithelial brush border lining the crypt lumen was visualized with rhodamine phalloidin. **C:** Bottleneck widths (mean ± SEM) in hatchling, 48-h aposymbiotic, and 48-h symbiotic animals, revealing both developmental and symbiosis-induced narrowing of this feature. Data shown represent 14–22 animals for each timepoint under each symbiotic condition, as all three bottlenecks could not always be clearly visualized in every animal. AC1, antechamber of crypt 1; BN1, BN2, BN3, bottleneck of crypt 1, 2, 3; DC1, deep crypt 1.

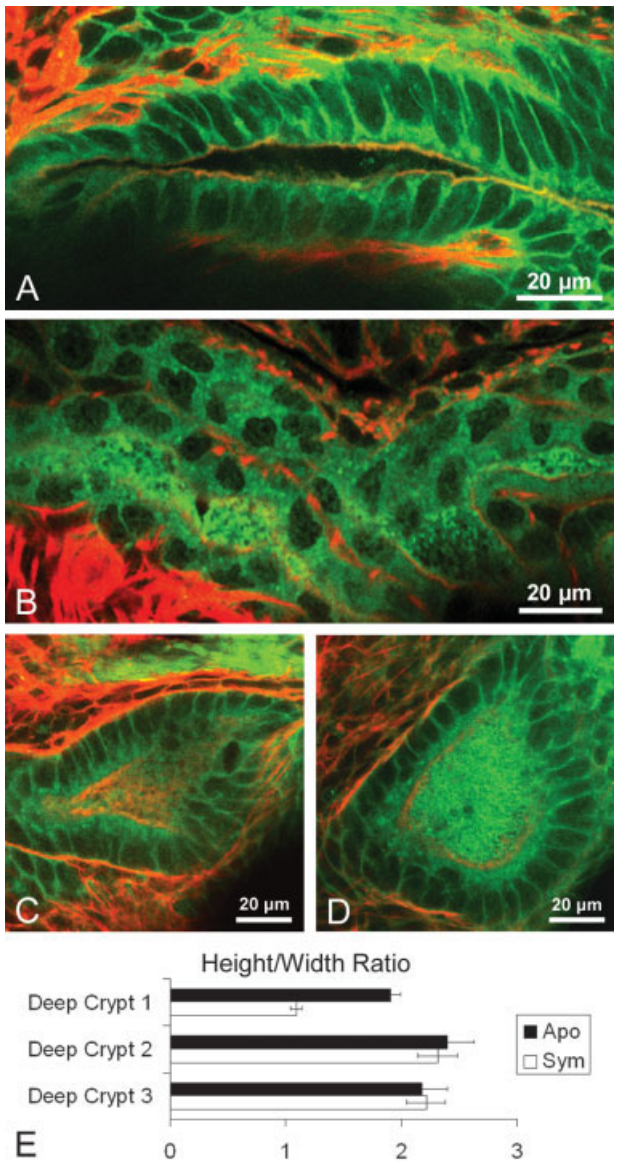

Fig. 6. Symbiosis-induced shape change in deep-crypt epithelial cells. Filamentous actin and cytoskeletal tubulin were stained with rhodamine phalloidin and BODIPY-FL paclitaxel, respectively, to visualize the crypt epithelial cells. **A:** Deep crypt 1 of a 48-h aposymbiotic animal. **B:** Deep crypt 1 of a 48-h symbiotic juvenile *Euprymna scolopes* colonized with GFP-labeled *Vibrio fischeri*. **C:** Deep crypt 3 of a 48-h aposymbiotic animal. **D:** Deep crypt 3 of a 48-h symbiotic animal colonized with GFP-labeled *V. fischeri*. **E:** Cell shape, characterized by the ratio of height to width (height/width or H/W), was either cuboidal (H/W ~1) or columnar (H/W ~2). Data are the means ± SEM from one of three replicate cell morphology experiments performed. The data summarize measurements from 3–4 aposymbiotic and symbiotic animals from a single clutch (DC1 n = 30 cells/animal, DC2/3 n = 5 cells/animal).

DISCUSSION

The results of this study reveal a hitherto unknown degree of structural complexity in the light organ crypts of juvenile *Euprymna scolopes*. Previous studies, using light microscopy and transmission electron microscopy (TEM), were able to resolve only two major divisions of each crypt: the ciliated duct, which terminates laterally at the pore that opens into the mantle cavity, and the medial blind-ended lumen, lined by nonciliated cells, where the bacterial symbionts were reported to colonize (Montgomery and McFall-Ngai, 1993, 1994). Viewing the light organs with confocal microscopy has revealed two additional features. Located immediately medial to the duct is a region we termed the "antechamber," which is more cavernous than the duct, but, like the duct, appears to be ciliated. Connecting the medial end of the antechamber to the deep crypt region is another tube-like feature that we designated the "bottleneck" because of its strikingly narrow diameter. Examination of the deep crypt areas also revealed a greater morphological complexity than had been previously observed. In summary, each crypt is now known to consist of four regions: duct, antechamber, bottleneck, and deep crypt. In addition, the present study provides a more precise view of the differences among the trio of crypts found on each side of the juvenile light organ, as well as the influence of the bacterial symbionts on the development of the crypt morphology and anatomy.

Insights Into Crypt Function

The new understanding of crypt structure provided by confocal microscopy suggests several new questions about how the crypts function in the early stages of the symbiosis. Among these questions are: what role, if any, does the antechamber play in bacterial colonization and/or persistence? Despite its significant volume, once the light organ is colonized the antechamber remains devoid of bacteria, except around the time of the daily dawn venting process. A recent study (Davidson et al., 2004) that was informed by this new understanding of crypt anatomy revealed that the duct and antechamber, but not the bottleneck or deep crypts, of hatchling and aposymbiotic animals produce high levels of nitric oxide (NO), a potent microbicide. Thus, with their ciliary activity (McFall-Ngai and Ruby, 1998) and NO production, these data suggest that the ducts and antechambers present both a biomechanical and a biochemical barrier through which *Vibrio fischeri* cells must pass before they can colonize the deep crypts. As such, these regions may play a major role in determining symbiont specificity by creating an environment that is permissive only to *V. fischeri.* Alternatively, these impediments to bacterial colonization could function to control the location and/or level of symbiont proliferation. Previous studies have shown that the onset of deep-crypt colonization by *V. fischeri* results in a significant attenuation of NO production in the more-laterally located duct and antechamber regions (Davidson et al., 2004). Thus, the ability of *V. fischeri* to not only move through, but also persist within, the crypts may be

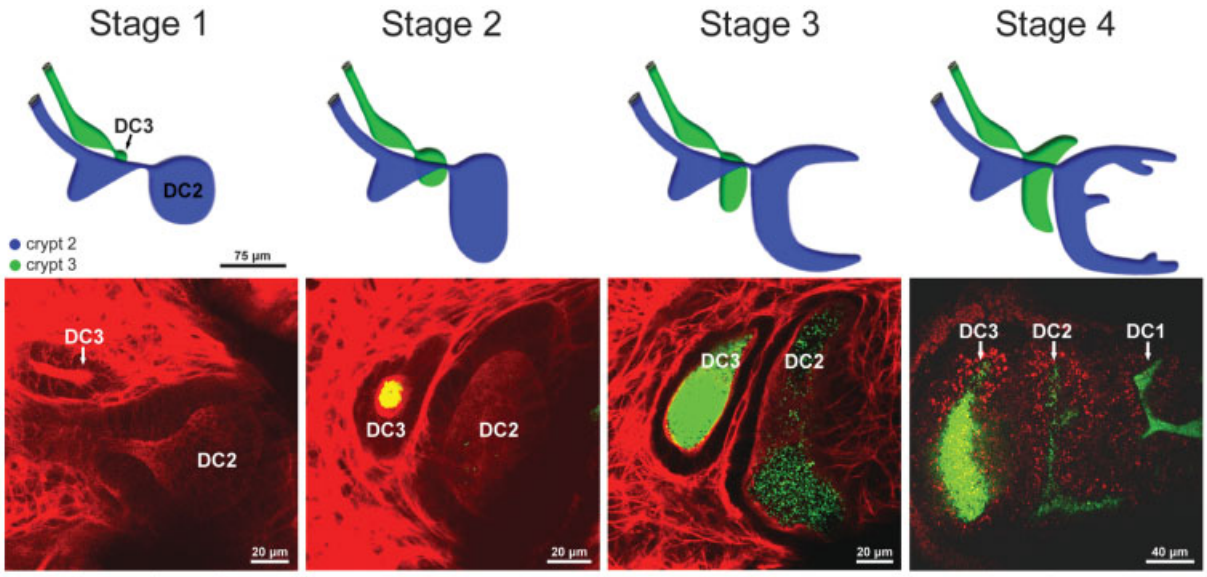

hatching	24 hrs	48 hrs	72 hrs
70.0%	31.3%	15.4%	16.7%

hatching	24 hrs	48 hrs	72 hrs
10.0%	50.0%	61.5%	41.7%

hatching	24 hrs	48 hrs	72 hrs
20.0%	18.8%	15.4%	33.3%

hatching	24 hrs	48 hrs	72 hrs
0%	0%	7.7%	8.3%

Fig. 7. Variation in, and developmental progression of, deep crypts 2 and 3 during the first 72 h postcolonization. Diagrams of the observed morphologies (Stages 1–4, from least to most developed), illustrating variations in the relative size and degree of complexity of deep crypts 2 (DC2) and 3 (DC3). The micrographs below each diagram provide examples of each developmental stage and morphology as observed by confocal microscopy. The GFP-labeled symbionts were observed colonizing these two deep crypt regions only in their more developed stages. *Euprymna scolopes* tissues are stained with rhodamine phalloidin or CellTracker Orange. The tables (bottom) present the frequency with which a given morphology was observed at a specific timepoint. The highlighted box (yellow) indicates the timepoint at which a particular morphology was most frequently seen. Table data were derived by counting the observed morphologies in symbiotic animals from four clutches (n = 10–16 animals/timepoint). DC1, DC2, DC3, deep crypts 1, 2, 3.

due, at least in part, to its ability to attenuate NO production in the ducts and antechambers. It is important to note that the antechamber may have additional but as yet unknown functions in the early stages of light organ development, a possibility supported by the size and distinct morphology of this structure.

The newly defined bottleneck region of the crypt is of particular structural interest because it forms a constricted passageway that separates the uncolonized duct/antechamber region from the colonized deep-crypt lumen. Its dimensions suggest that the bottleneck serves as a physical obstacle to bacteria or other materials trying to enter the deep crypt. In our observations of primary colonization, while the bottleneck certainly appeared to limit the rate at which large bacterial populations passed from the antechamber to the deep crypt, individual symbionts were in no way blocked, and could move through the passageway in a column several cells wide. However, as a result of colonization the bottleneck further narrows to nearly the width of a single bacterial cell (Fig. 5), thereby presenting a more substantial physical barrier to bacteria both entering and leaving the deep crypt. Thus, the bottleneck may facilitate the containment of *Vibrio fischeri* cells in the deep crypts at times of day other than venting. In addition, because the pores remain open to the external environment throughout the life of the host, this narrow passageway may also limit subsequent colonization by additional *V. fischeri* strains or nonsymbiotic bacterial species. One additional issue that will require further investigation is how the bacteria overcome the obstacle of the bottleneck so rapidly during venting. Are they simply forced through the narrow passage by the powerful light-organ musculature (Nyholm and McFall-Ngai, 1998), or does the width of the bottleneck change with a diel rhythm?

Juvenile Crypt Development

Although the four morphological regions are identifiable within all of the six juvenile crypts, their relative sizes and precise morphologies differ between the three pairs (Fig. 7). Studies of the adult squid reported that the mature crypts differ slightly in size, with crypt 1 being the largest and crypt 3 the smallest; nevertheless, they all share a similar branching structure (Montgomery and McFall-Ngai, 1998). Thus, maturation of the crypt spaces appears to involve continued growth and ramification of all three crypts that results in DC2 and DC3 following the progression of increasing size and complexity first displayed by DC1. We observed that DC2 and DC3 were, on average, slightly but significantly

larger in colonized animals. Because the rates of crypt cell proliferation in aposymbiotic and symbiotic animals do not differ (Montgomery and McFall-Ngai, 1994), we hypothesize that this symbiosis-associated increase in size results from a stretching of the crypt spaces imposed by the growing population of symbionts. Our studies of early deep-crypt development indicated that DC2 and DC3 continue to grow and branch toward the mid-line of the organ. Eventually, however, the continued growth of the crypts must be primarily in the anterior and posterior directions, as histological sections studies of the adult organ have shown that the mature crypts are elongated along this axis (Montgomery and McFall-Ngai, 1998).

Unlike the deep crypt regions, a significant preprogrammed developmental progression was not observed for the antechamber and bottleneck regions in the first 72 h after hatching (Fig. 7). More specifically, no change in cross-sectional size or shape of the antechambers was measurable over the first 72 h; i.e., AC3 did not begin to assume the stomach-like shape of AC1 and AC2. Although the eventual fate of the antechamber is not readily discernable by examination of the adult light organ, one possible fate of AC1 and AC2 is that they may develop into the two yellow-pigmented diverticula of the adult crypts, which are positioned just medial to the single adult duct, and have the same general shape as the antechambers (Montgomery and McFall-Ngai, 1998). These yellow pads of tissue in the adult organ occur over the ventral surface of the crypt region and are of unknown function. Results from a previous study (Weis et al., 1993) links the antechambers with these pigmented areas. Specifically, high levels of the enzyme aldehyde dehydrogenase are produced in these regions in adults, and the first developmental signs of this biochemical signature occur at the crypt–duct interface in juvenile animals, i.e., in the same location as the area now known to be the antechamber (Weis et al., 1993). In addition to finding no marked development changes in the antechambers, although symbiosis-induced bottleneck constriction was noted during this time, we did not detect significant elongation of the bottleneck during the first 72 h after hatching. However, histological sections of adult light organs suggest that the bottlenecks later elongate into narrow passages of up to 250 μm in length that connect the deep crypts with the duct region of the crypts (Montgomery and McFall-Ngai, 1998).

Role of the Symbionts in Light-Organ Morphology

Our investigation unexpectedly revealed functional variation among the three deep-crypt areas that sheds new light on this region's dynamic role in the symbiosis. Two unanticipated observations were 1) the incomplete venting of bacteria from DC2 and DC3, and 2) the failure of colonization to induce an expected morphological change in the epithelial cells lining DC2 and DC3. In both cases the development of these deep-crypt regions failed to duplicate the patterns that were first described for DC1, which had been assumed to be emblematic of normal symbiotic function (Graf and Ruby, 1998; Visick et al., 2000). Do these different cellular responses to the symbionts reflect distinct functionality among the different crypts, or are the differing cell morphologies simply a consequence of the relative developmental immaturity of DC2 and DC3?

The diel venting of ~90% of the crypt's contents each morning is believed to enable the squid to foster the regrowth of a fresh, metabolically robust, symbiont population that will efficiently luminesce through the coming night (Graf and Ruby, 1998). It was initially assumed that this behavior was characteristic of all of the crypts, but the present study has revealed that the three pairs of crypts are unequal in the extent to which they vent (e.g., Fig. 4F). Because all three crypts were capable of at least partial expulsion, and their relative extent of venting coincided with the order in which they developed (i.e., DC1 > DC2 > DC3), a parsimonious explanation would be that the observed differences are due to a developmental immaturity of the contractile tissues around the younger crypts. Similarly, differences in the extent of venting could also be a consequence of position; DC3 is the most lateral, DC1 is the most medial, and DC2 is in between (Fig. 1C). It is possible that, because it is most laterally located relative to the medial musculature of the light organ and ink sac, the juvenile DC3 vents poorly due to the lack of direct contractile force (Nyholm and McFall-Ngai, 1998). Measurements of the extent of venting behavior in the crypts of more mature squid, coupled with a better understanding of the biomechanics of venting, will help discriminate between these hypotheses. In any case, an accessible population of crypt-grown, nonvented symbionts in DC3 provides an opportunity to better understand the reason for the venting behavior itself.

While a previous study reported that the epithelia lining the deep portion of crypt 3 were not significantly different between aposymbiotic and symbiotic animals at 3 days posthatch, crypt 3 had not become colonized by that time (Montgomery and McFall-Ngai, 1994). Because swelling of the deep crypt epithelia, and the associated change from a columnar to a cuboidal cell shape, apparently require the presence of colonizing symbionts (Visick et al., 2000), it is possible to explain the failure of the epithelium to respond in that study by the absence of colonizing bacteria in that particular crypt. In contrast, in our experiments, performed with a different population of *Euprymna scolopes* than the earlier study (Kimbell et al., 2002), crypt 3 was nearly always mature enough to become colonized immediately after hatching and continually support a dense popula-

tion of symbiotic bacteria (Fig. 3). Nevertheless, as late as 48 h posthatch the epithelial cells of DC3, and often DC2 as well, had not changed to a cuboidal shape observed in the cells of DC1.

The absence of this response in DC2 and DC3 is significant because it has been suggested that the cell swelling underlying this change in morphology reflects the stress imposed by metabolic and oxidative activity of the symbiont population (Ruby and McFall-Ngai, 1999). Why then do the epithelial cells of DC2 and DC3, which are in contact with a large number of apparently active symbionts, not show this morphological response? We hypothesize that the ability to initiate this response develops somewhat after the capacity to support a symbiotic population. Only the more mature and possibly fully differentiated epithelia of DC1 reliably express this response, whereas the comparatively immature and still dividing epithelia of DC2 and DC3 (Montgomery and McFall-Ngai, 1994) are incapable. Our observation of a partial degree of swelling in DC2 in one experiment (Fig. 6), as well as a previous report of the DC3 epithelia appearing cuboidal in an older juvenile (Montgomery and McFall-Ngai, 1994), supports this notion. However, further investigation will be needed to test whether, upon reaching a more advanced state of maturity, the epithelia of DC2 and DC3 become able to fully respond to the colonizing symbionts.

The application of confocal microscopy not only allowed us to better view the 3D complexity of the symbiotic light organ of *Euprymna scolopes*, but also to compare the sizes of structures and the relationships of tissues in both living and fixed specimens. This capability was critical to determining whether the fixation process itself was introducing morphological artifacts. Our data revealed that, under confocal microscopy, fixation did not markedly perturb the tissue or affect our conclusions. Such comparative analyses of living and fixed tissues have not been possible with the light and electron microscopy studies of squid light organs that have been previously reported (Herring et al., 1981; Montgomery and McFall-Ngai, 1993, 1994, 1998; Nishiguchi et al., 2004). In addition, previously reported TEM-based, 3D reconstructions of the juvenile light organ (Montgomery and McFall-Ngai, 1993) did not reveal the narrow bottleneck, a critical component of the crypt anatomy described here using confocal analyses. We predict that the application of confocal microscopy, in conjunction with light and electron microscopy, will continue to uncover the true relationship of the tissues of the squid light organ, producing an invaluable framework in which to study developmental and functional aspects of this symbiosis.

ACKNOWLEDGMENTS

We thank Tanya Koropatnick, Debbie Millikan, Spencer Nyholm, and Cheryl Whistler for insight and assistance with this work.

LITERATURE CITED

Arnold JM, Singley C, Williams-Arnold L. 1972. Embryonic development and post-hatching survival of the sepiolid squid *Euprymna scolopes* under laboratory conditions. Veliger 14:361–364.

Boettcher KJ, Ruby EG. 1990. Depressed light emission by symbiotic *Vibrio fischeri* of the sepiolid squid *Euprymna scolopes*. J Bacteriol 172:3701–3706.

Boettcher KJ, Ruby EG, McFall-Ngai MJ. 1996. Bioluminescence in the symbiotic squid *Euprymna scolopes* is controlled by a daily biological rhythm. J Comp Physiol [A] 179:65–73.

Claes MF, Dunlap PV. 2000. Aposymbiotic culture of the sepiolid squid *Euprymna scolopes*: role of the symbiotic bacterium *Vibrio fischeri* in host animal growth, development, and light organ morphogenesis. J Exp Zool 286:280–296.

Davidson SK, Koropatnick TA, Kossmehl R, Sycuro L, McFall-Ngai MJ. 2004. NO means 'yes' in the squid-vibrio symbiosis: nitric oxide (NO) during the initial stages of a beneficial association. Cell Microbiol 6:1139–1151.

Doino JA, McFall-Ngai MJ. 1995. A transient exposure to symbiosis-competent bacteria induces light organ morphogenesis in the host squid. Biol Bull 189:347–355.

Graf J, Ruby EG. 1998. Host-derived amino acids support the proliferation of symbiotic bacteria. Proc Natl Acad Sci U S A 95:1818–1822.

Herring PJ, Clarke MR, Boletzky SV, Ryan KP. 1981. The light organs of *Sepiola atlantica* and *Spirula spirula* (Mollusca: Cephalopoda): bacterial and intrinsic systems in the order Sepiodea. J Mar Biol Assoc UK 61:901–916.

Kimbell JR, McFall-Ngai MJ. 2004. Symbiont-induced changes in host actin during the onset of a beneficial animal-bacterial association. Appl Environ Microbiol 70:1434–1441.

Kimbell JR, McFall-Ngai MJ, Roderick G. 2002. Two genetically distinct populations of *Euprymna scolopes* in the shallow waters of Oahu, Hawaii. Pac Sci 56:347–355.

Lamarcq LH, McFall-Ngai MJ. 1998. Induction of a gradual, reversible morphogenesis of its host's epithelial brush border by *Vibrio fischeri*. Infect Immun 66:777–785.

McFall-Ngai MJ, Ruby EG. 1991. Symbiont recognition and subsequent morphogenesis as early events in an animal-bacterial mutualism. Science 254:1491–1494.

McFall-Ngai MJ, Ruby EG. 1998. Sepiolids and vibrios: when first they meet. BioScience 48:257–265.

Montgomery MK, McFall-Ngai M. 1993. Embryonic development of the light organ of the sepiolid squid *Euprymna scolopes* Berry. Biol Bull 184:296–308.

Montgomery MK, McFall-Ngai M. 1994. Bacterial symbionts induce host organ morphogenesis during early postembryonic development of the squid *Euprymna scolopes*. Development 120:1719–1729.

Montgomery MK, McFall-Ngai MJ. 1998. Late postembryonic development of the symbiotic light organ of *Euprymna scolopes* (Cephalopoda:Sepiolidae). Biol Bull 195:326–336.

Moynihan M. 1983. Notes on the behavior of *Euprymna scolopes* (Cephalopoda: Sepiolidae). Behaviour 85:25–41.

Nishiguchi MK, Lopez JE, Boletzky Sv. 2004. Enlightenment of old ideas from new investigations: more questions regarding te evolution of bacteriogenic light organs in squids. Evol Dev 6:41–49.

Nyholm SV, McFall-Ngai MJ. 1998. Sampling the light-organ microenvironment of *Euprymna scolopes*: description of a population of host cells in association with the bacterial symbiont *Vibrio fischeri*. Biol Bull 195:89–97.

Nyholm SV, McFall-Ngai MJ. 2003. Dominance of *Vibrio fischeri* in secreted mucus outside the light organ of *Euprymna scolopes*: the first site of symbiont specificity. Appl Environ Microbiol 69:3932–3937.

Nyholm SV, McFall-Ngai MJ. 2004. The winnowing: establishing the squid-vibrio symbiosis. Nat Rev Microbiol 2:632–642.

Nyholm SV, Stabb EV, Ruby EG, McFall-Ngai MJ. 2000. Establishment of an animal-bacterial association: recruiting symbi-

otic vibrios from the environment. Proc Natl Acad Sci U S A 97:10231–10235.

Nyholm SV, Deplancke B, Gaskins HR, Apicella MA, McFall-Ngai MJ. 2002. Roles of *Vibrio fischeri* and nonsymbiotic bacteria in the dynamics of mucus secretion during symbiont colonization of the *Euprymna scolopes* light organ. Appl Environ Microbiol 68:5113–5122.

Ruby EG, Lee K-H. 1998. The *Vibrio fischeri-Euprymna scolopes* light organ association: current ecological paradigms. Appl Environ Microbiol 64:805–812.

Ruby EG, McFall-Ngai MJ. 1999. Oxygen-utilizing reactions and symbiotic colonization of the squid light organ by *Vibrio fischeri*. Trends Microbiol 7:414–420.

Visick KL, Foster J, Doino J, McFall-Ngai M, Ruby EG. 2000. *Vibrio fischeri lux* genes play an important role in colonization and development of the host light organ. J Bacteriol 182:4578–4586.

Weis VM, Montgomery MK, McFall-Ngai MJ. 1993. Enhanced production of ALDH-like protein in the bacterial light organ of the sepiolid squid *Euprymna scolopes*. Biol Bull 184:309–321.